(Submitted to Physics Letters B)

Study of the Energy and Charged Multiplicity Dependence of Inclusive π^- Production in π^-p Interactions Up to Fermilab Energies

W. Morris, B. Y. Oh, D. L. Parker, G. A. Smith, J. Whitmore,
L. Voyvodic, R. Walker, R. Yaari, E. W. Anderson, H. B. Crawley,
W. J. Kernan, F. Ogino, R. G. Glasser, D. G. Hill, G. McClellan,
H. L. Price, B. Sechi-Zorn, G. A. Snow, F. Svrcek, W. D. Shephard,
J. M. Bishop, N. N. Biswas, N. M. Cason, E. D. Fokitis and V. P. Kenney

Michigan State University, East Lansing, Michigan 48824*
Fermi National Accelerator Laboratory, Batavia, Illinois 60510#
Iowa State University and Ames Laboratory, ERDA, Ames, Iowa 50010#
University of Maryland, College Park, Maryland 20742#
University of Notre Dame, Notre Dame, Indiana 46556*

ABSTRACT

Using new data from 100 GeV/c π^-p interactions, we find the energy dependence of the invariant cross-section in the target fragmentation (central) region to be consistent with an $A + Bs^{-1/2}$ $(C + Ds^{-1/4})$ behavior. The leading particle peak near x=+1 exhibits a width in x which becomes smaller with increasing energy and an integrated cross section which is approximately energy independent.

---

*Research supported in part by the National Science Foundation
#Research supported in part by the U.S. Energy Research and Development Administration.

Since the initial operation of the CERN ISR and Fermilab, much has been learned from inclusive single particle distributions. For example, proton diffractive excitation has been studied by measuring the mass recoiling from the proton in the reaction $pp \to p + \text{anything}$. Such experiments[1] have shown that (1) masses as high as 5 GeV may be excited, (2) the typical multiplicity of secondary charged particles is less than the overall average multiplicity, and (3) this diffractive multiplicity increases with increasing mass. Similar features have been observed for pion dissociation in the reaction

$$\pi^- p \to p + \text{anything} \qquad (1)$$

at 205 GeV/c.[2] We present the first measurement above 40 GeV/c of the inclusive π^- invariant cross section for the complementary reaction

$$\pi^- p \to \pi^- + \text{anything}. \qquad (2)$$

These new data provide additional information[2,3] on reactions (1) and (2), and when combined with lower energy results provide information on the energy dependence of inclusive π^- production in the central region and in the beam and target fragmentation regions.

The data consist of 3730 events from 65,000 pictures of 100 GeV/c $\pi^- p$ interactions in the Fermilab 30-inch bubble chamber with four downstream wide-gap optical spark chambers. On typical secondary tracks this system yields a $\Delta p/p \sim \pm(4 \times 10^{-4})p$ (GeV/c). Accordingly, we can study reaction (2) for all π^- angles and momenta and for all charged particle multiplicities of the recoiling system. After determining elastic events by kinematic fits, the resulting inelastic and elastic cross sections are in good agreement with previously determined values.[4] All negative particles are assumed to be π^- and protons with laboratory momenta less than 1.4 GeV/c have been identified by ionization. In the beam fragmentation region, $x \geq +0.55$ ($x = 2P_L^*/\sqrt{s}$),

we use only tracks with complete bubble chamber-spark chamber information. Since some of the fast forward-going tracks interact in the bubble chamber windows, it has been necessary to correct for these losses. The overall normalization of the data is obtained from published topological cross sections.[4]

Figure 1 shows the inelastic differential cross-section for inclusive π^- production. It is well known that $\pi^-(\pi^+)$ produced in π^-p (π^+p) interactions at incident momenta below 50 GeV/c exhibit definite "leading particle" effects; that is, the $\pi^-(\pi^+)$ production in the beam fragmentation CM hemisphere is greatly enhanced over that observed in the target hemisphere. Furthermore, $\pi^\pm p$ experiments[5] at 16 GeV/c observe a peak in the inelastic $\pi^\pm$ invariant cross-section near x=+1. Figure 1 shows that the asymmetry is still a dominant feature at 100 GeV/c. In addition, we see a significant peak near x=+1. In comparison, the lower energy data[6,7] show only a broad shoulder[8] between x=+0.5 and x=+1.0. Figure 1 also indicates that the cross-section in the target fragmentation region ($x \lesssim -0.2$) is falling[9] between 18.5 and 100 GeV/c.

To investigate the multiplicity dependence, we show in Figure 2 the semi-inclusive distributions. Both the 2 and 4 prong data show a peak near x=+1. The 6 prong data (not shown) show no evidence for such a narrow peak. Figure 2(b) also shows (shaded area) the π^- distribution from 4-prong events which fit the reaction $\pi^-p \to \pi^-p\pi^+\pi^-$. A large fraction (~46%) of the peak for $x > +0.8$ is due to this reaction. This demonstrates that the diffractive excitation process occurs primarily in final states with low total multiplicity. Figure 2 also shows data at 18.5[6] and 150 GeV/c[3]. It is interesting to note the absence of a peak near x=+1 in the low energy semi-inclusive

4-prong data. We note that the integrated 2(4) prong cross section varies from 4.8 ± 0.4 (9.17 ± 0.25)mb at 18.5 GeV/c to 1.95 ± 0.29 (4.79 ± 0.11)mb at 100 GeV/c. These variations account for the differences near x=0.

We determine cross-sections for proton diffractive excitation, p*, [in reaction (2)] by estimating the numbers of events above hand-drawn backgrounds, such as those shown in Figures 1 and 2. The results are given in Table I, where they are compared to the cross-sections for pion excitation, π^{-*}, as determined from reaction (1) in this experiment. The errors given in Table I include statistical and normalization uncertainties arising from background and, for the 2-prongs, from the elastic-inelastic separation. The dominant features of these cross sections are that (a) they are consistent with values at other energies[2,3,7] and (b) the ratio $R_1 = \sigma(\pi^- p \to p^*)/\sigma(\pi^- p \to \pi^{-*})$ is consistent with unity for each charged multiplicity.[3]

The proton excitation data may be used to test Pomeron factorization by comparison with similar data from pp interactions. Table I shows values of $R_2 = \sigma(\pi^- p \to p^*)\cdot\sigma_{el}(pp)/\sigma(pp \to p^*)\cdot\sigma_{el}(\pi^- p)$. We note that factorization ($R_2 = 1$) is satisfied to about one standard deviation, although all three individual measurements give R_2 greater than unity.

In Figure 3(a) we show the inclusive π^- invariant cross-section, $F(x) = \int (2E/\pi\sqrt{s})\ (d^2\sigma/dx dP_T^2) dP_T^2$. The charged multiplicity dependence, shown in Figures 3(b-d), illustrates features similar to those observed in Fig. 2. The peak near x=+1 is clearly visible only in the inelastic two- and four-prong data. In addition, the six-prong cross-section for $x \gtrsim +0.5$ is rising with increasing energy.

By comparison with data at 16 and 18.5 GeV/c, the 100 GeV/c data indicate that the inclusive cross section in the target fragmentation region

($x \leq -0.2$) continues to fall with increasing energy.[10] Fig. 4(a) shows[11] the structure function, $G(P_L) = \int (E/\sigma_T)\ (d^2\sigma/dP_L dP_T^2) dP_T^2$, evaluated in the laboratory and integrated over all backward angles, with σ_T = 24.9 mb. The energy dependence[12] is consistent with an approach to the scaling limit as $A + Bs^{-1/2}$. Presumably the nonzero value of A arises from a contribution from the energy independent p* diffractive dissociation cross section. Furthermore, these data are consistent with an infinite energy limit, A, which is independent of the charge of the beam pion.

Figure 3(a) also shows that the cross section at x=0 rises with increasing energy. Figure 4(b) shows[7,10,11] the invariant structure function $F(o)/\sigma_T$ (averaged for $|x| \leq 0.02$) as a function of $s^{-1/4}$. The trend of the $\pi^- p \to \pi^-$ data has changed from one showing little variation to one increasing with energy, and at very high energies the cross section at x=0 may be independent of the charge of the incident pion beam.

Finally, when compared to the 16 GeV/c spectra,[5] these Fermilab data on the peak near x=+1 (see Fig. 3(a)) show that with increasing energy (a) the peak cross-section varies slowly, and (b) the width of the peak appears to decrease. It is interesting to note that features very similar to these are also observed[1] in the inclusive proton spectra from pp collisions at these energies.

REFERENCES

1. J. Whitmore, Phys. Reports, 10C (1974) 273.
2. F. C. Winkelmann et al., Phys. Rev. Letters 32 (1974) 121.
3. D. G. Fong, et al., Phys. Letters 53B (1974) 290.
4. E. L. Berger, Nucl. Phys. B77 (1974) 365.
5. P. Bosetti et al., Nucl. Phys. B54 (1973) 141.
6. J. T. Powers et al., Phys. Rev. D8 (1973) 1947; P. T. Go and W. D. Shephard, private communication.
7. E. O. Abdrakhmanov et al., Nucl. Phys. B72 (1974) 189; N. Angelov et al., JINR preprint P1-7924 (1974); V. Grishin, private communication.
8. It is estimated that $\Delta\bar{x}/x$ near x=+1 in the 18.5 GeV/c data is comparable to that at 100 GeV/c. However, the resolution in the 40 GeV/c data (Ref. 7) is substantially poorer ($\gtrsim$ 12%).
9. The 40 GeV/c data (Ref. 7), obtained in a propane bubble chamber, are inconsistent with the 18.5 and 100 GeV/c data for $x < -0.2$. In view of the problems inherent in experiments with nonhydrogen events, we do not use these data in the ensuing discussion of the energy dependence of this x region.
10. M. Alston-Garnjost et al., Phys. Letters 39B (1972) 402.
11. W. D. Shephard et al., Paper #760, XVII Inter. Conf. on H.E.P. (London, 1974); J. Erwin et al., Phys. Rev. Letters 33 (1974) 1355.
12. A. H. Mueller, Phys. Rev. D2 (1970) 2963.

Table I. Cross Sections for Single Diffractive Excitation (mb)

n_c	π^{-*}	p^*	R_1[a]	R_2[a,b]
2	0.50 ± 0.07	0.84 ± 0.12	1.68 ± 0.34	1.57 ± 0.40
4	0.79 ± 0.07	0.74 ± 0.15	0.94 ± 0.21	1.50 ± 0.46
6	0.28 ± 0.08	0.33 ± 0.12	1.18 ± 0.55	2.89 ± 1.56
8	0.06 ± 0.03	0.09 ± 0.09	1.5 ± 1.5	--
Total	1.63 ± 0.13	2.00 ± 0.21	1.23 ± 0.16	1.75 ± 0.31

[a] See text for definitions of R_1 and R_2.

[b] See Ref. (1) for $\sigma(pp \to p^*)$.

FIGURE CAPTIONS

Fig. 1 The inclusive cross-section, $d\sigma/dx$. The curve is our estimate of the nondiffractive background.

Fig. 2 $d\sigma/dx$ for (a) inelastic two-prong and (b) four-prong events. The shaded events give good 4C fits. The curves are as defined in Figure 1.

Fig. 3 The π^- invariant cross section for (a) inclusive; (b) inelastic two-prong; (c) four-prong; and (d) six-prong events.

Fig. 4 (a) $\int_{-0.4}^{0} G(P_L)dP_L$ as a function of $s^{-1/2}$; (b) $F(o)/\sigma_T$, as a function of $s^{-1/4}$. The solid curves are hand-drawn to guide the eye.

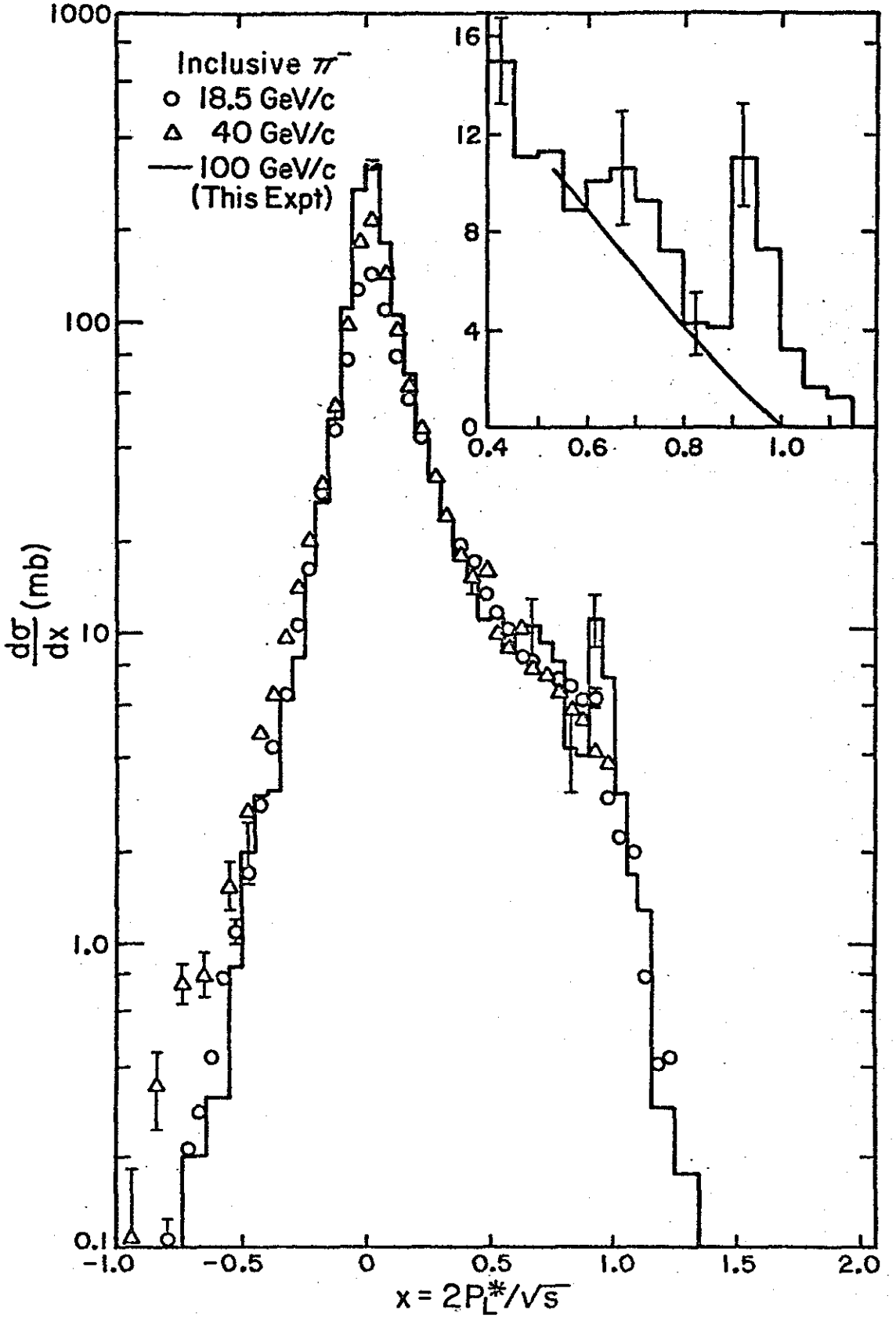
Inclusive π^-
o 18.5 GeV/c
Δ 40 GeV/c
— 100 GeV/c
(This Expt)
$\frac{d\sigma}{dx}$ (mb)
$x = 2P_L^*/\sqrt{s}$
1000
100
10
1.0
0.1
-1.0
-0.5
0
0.5
1.0
1.5
2.0
16
12
8
4
0
0.4
0.6
0.8
1.0

Figure 1

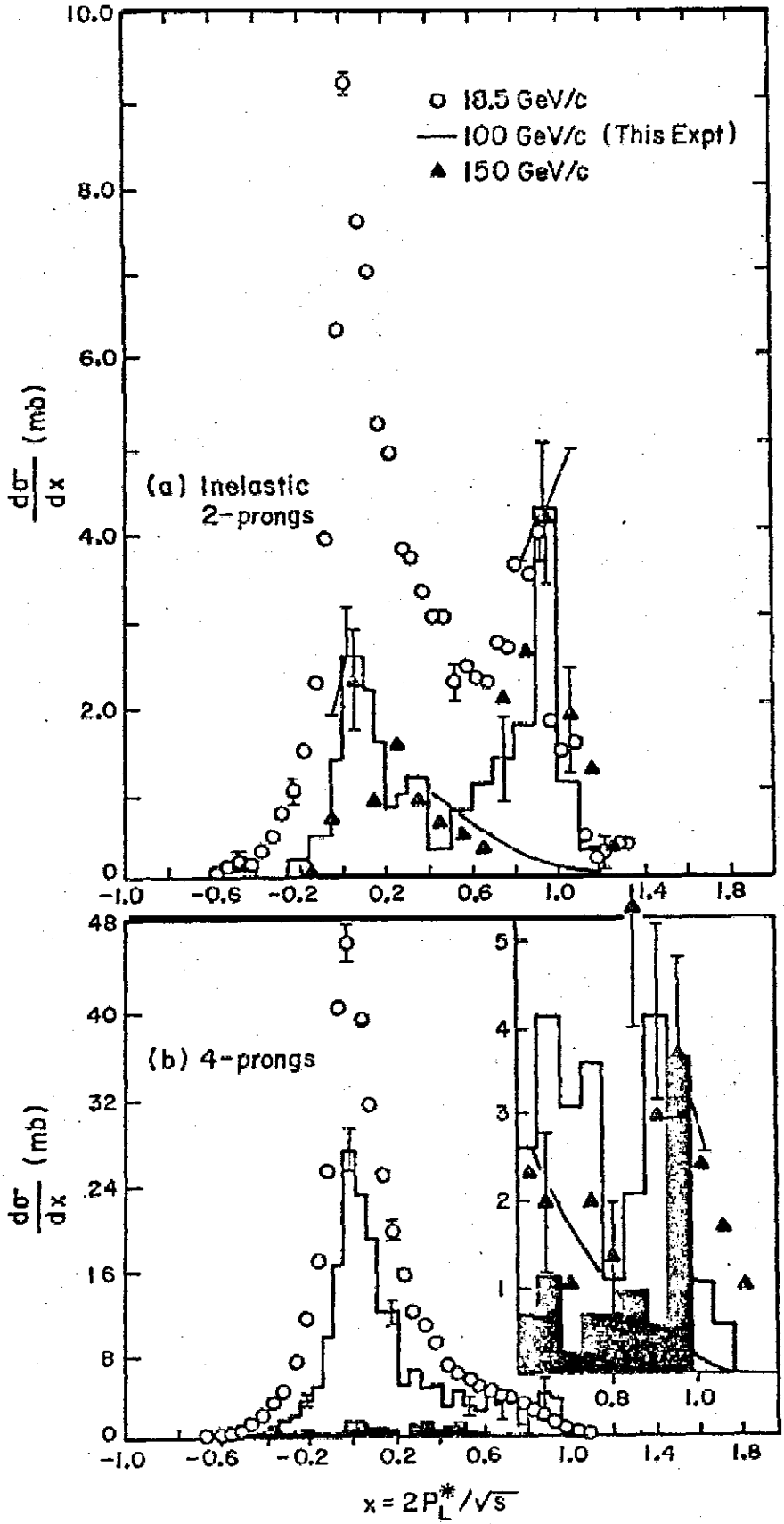
18.5 GeV/c
100 GeV/c (This Expt)
150 GeV/c
(a) Inelastic 2-prongs
(b) 4-prongs
dσ/dx (mb)
x = 2P*L/√s

Figure 2

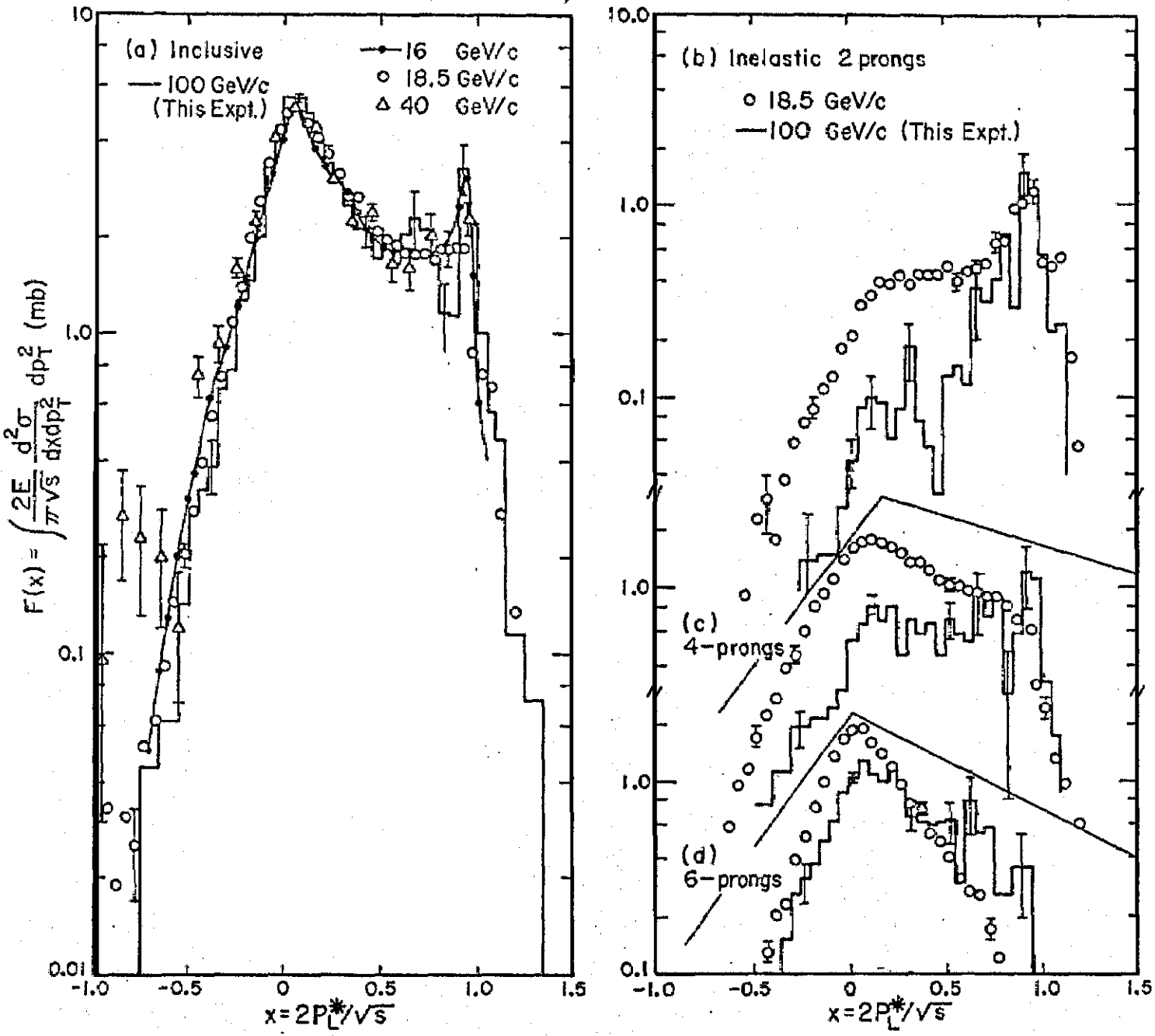
(a) Inclusive
100 GeV/c (This Expt.)
16 GeV/c
18.5 GeV/c
40 GeV/c
$F(x) = \int \frac{2E}{\pi\sqrt{s}} \frac{d^2\sigma}{dx dp_T^2} dp_T^2$ (mb)
$x = 2P_L^*/\sqrt{s}$
(b) Inelastic 2 prongs
18.5 GeV/c
100 GeV/c (This Expt.)
(c) 4-prongs
(d) 6-prongs
$x = 2P_L^*/\sqrt{s}$

Figure 3

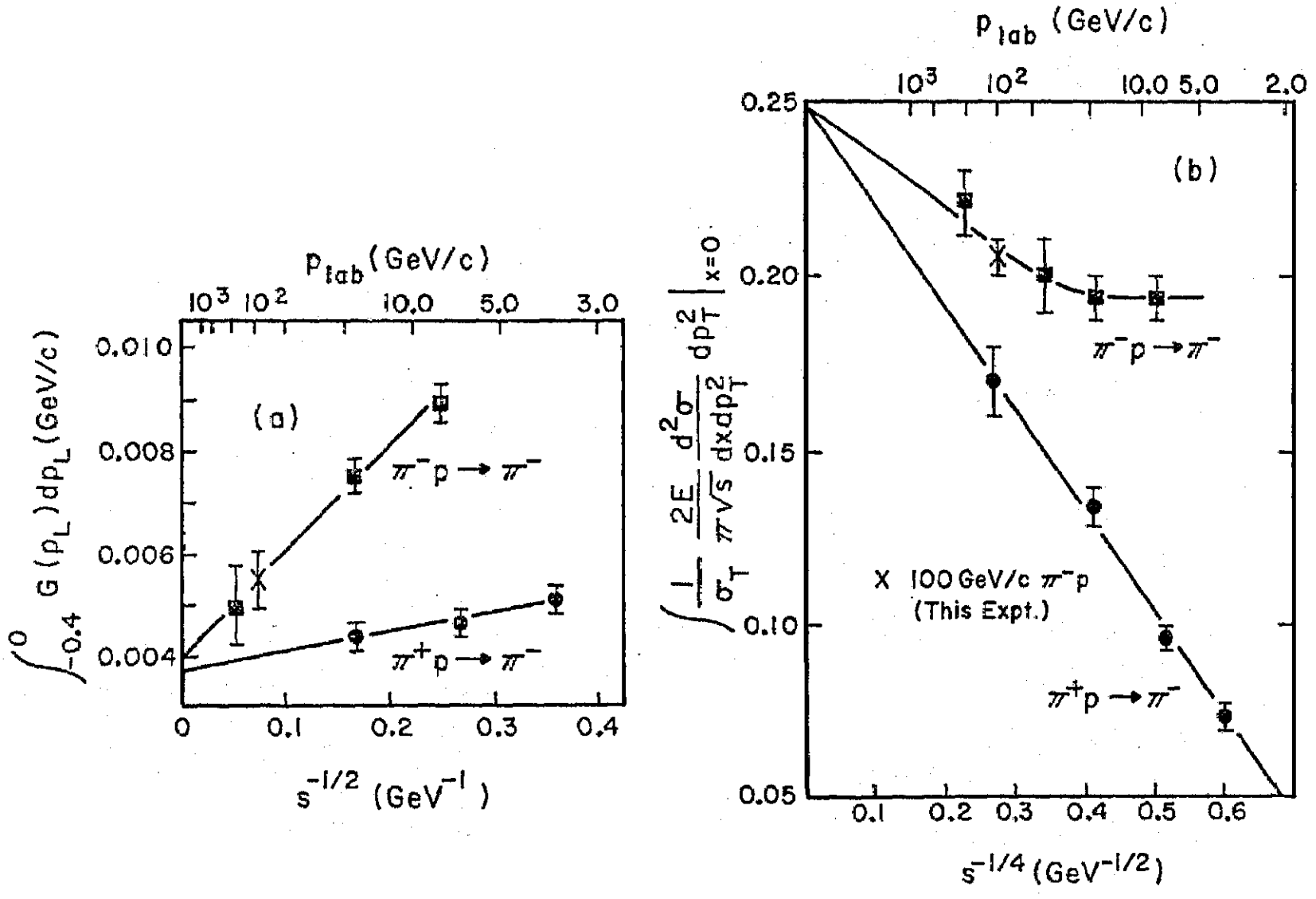
p lab (GeV/c)
10^3 10^2 10.0 5.0 3.0
0.010
0.008
0.006
0.004
(a)
π⁻p → π⁻
π⁺p → π⁻
0 0.1 0.2 0.3 0.4
s^-1/2 (GeV^-1)
∫ 0 -0.4 G(p_L) dp_L (GeV/c)
p lab (GeV/c)
10^3 10^2 10.0 5.0 2.0
0.25
0.20
0.15
0.10
0.05
(b)
π⁻p → π⁻
X 100 GeV/c π⁻p
(This Expt.)
π⁺p → π⁻
0.1 0.2 0.3 0.4 0.5 0.6
s^-1/4 (GeV^-1/2)
∫ 1/σ_T 2E/π√s d²σ/dx dp_T² dp_T² |x=0

Figure 4